



Effect of biomass-coal blending combustion on Pb transformation

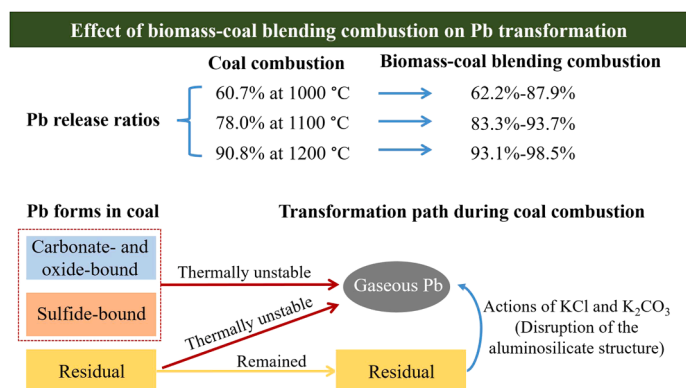
Xing-yu Yang, Guo-chang Song, Zhong-wei Li, Qiang Song^{*,1,2}

Key Laboratory of Thermal Science and Power Engineering of Ministry of Education, Department of Energy and Power Engineering, Tsinghua University, Beijing 100084, China

HIGHLIGHTS

- The effect of biomass-coal blending combustion on lead (Pb) transformation was studied.
- The release of Pb in coal was promoted during blending combustion.
- K compounds in biomass promoted the release of Pb, while Cl had little effect.
- K_2CO_3 and KCl could both react with aluminosilicate and release residual Pb.
- K_2CO_3 had a stronger promoting effect on Pb release than KCl.

GRAPHICAL ABSTRACT



ARTICLE INFO

Editor: John D Atkinson

Keywords:

Lead
Biomass
Coal
Blending combustion
Transformation

ABSTRACT

Biomass-coal blending combustion is an effective method for utilizing biomass; however, its pollutant emission requires attention. Herein, the effect of biomass-coal blending combustion on lead (Pb) transformation was explored. Combustion experiments were conducted in a fixed-bed reactor, using coal, corn stalk, rice stalk, bamboo flour and their mixtures as fuels, at 1000, 1100, 1200 and 1300 °C. The Pb release ratios were determined by measuring its content in the fuels and solid-phase combustion products. The distribution of Pb forms was analyzed using sequential chemical extraction. The results indicate that blending combustion significantly enhanced the release of Pb. At blending ratio 1:1, the release ratios increased by 1.54–27.2%, 5.30–15.6%, and 2.31–7.76% at 1000, 1100, and 1200 °C, respectively. The potassium (K) components in biomass, mainly KCl and K_2CO_3 , had a significant promoting effect on Pb release. K compounds facilitated the release of residual Pb through reactions with aluminosilicates. The promotion effect weakened as the temperature increased due to the faster evaporation rate of K. When the mass fractions of K in the fuels were equal, K_2CO_3 exhibited a stronger promoting effect. HCl had minimal impact on the transformation of Pb. The results are helpful for optimizing the combination of biomass and coal to control Pb emission from the blending combustion source.

* Correspondence to: Department of Energy and Power Engineering, Tsinghua University, Haidian District, Beijing 100084, China.

E-mail address: qsong@tsinghua.edu.cn (Q. Song).

¹ ORCID: 0000-0002-5484-3594

² Researcher ID: U-4938-2019

1. Introduction

Biomass is a significant renewable carbon source, distinguishing itself from other renewable energy sources. While it offers the advantage of reducing carbon emission and achieving neutrality, using biomass as the sole fuel presents challenges such as low combustion calorific value and ash accumulation [1,2]. Consequently, biomass-coal blending combustion emerges as a viable solution for biomass utilization [3,4]. Compared with sole coal combustion, biomass-coal blending combustion can reduce the emission of carbon dioxide, sulfur oxides, and nitrogen oxides. However, the relatively high contents of heavy metals in coal might bring new pollution concerns to biomass-coal blending combustion [5]. Among the heavy metals contained in coal, Pb is volatile with deleterious effects when released into the atmosphere from coal-fired systems [6,7]. Despite the presence of pollution control equipment, some power plants still exceed the emission standards set by the U.S. EPA [8,9]. Hence, the development of suitable control technologies to curtail Pb emission is imperative. Studying the distribution characteristics and transformation pathways of Pb during blending combustion can provide theoretical support for predicting and controlling Pb emission.

Pb release mainly originates from coal during biomass-coal blending combustion because the Pb content of biomass is much less than that of coal [10]. The transformation of Pb in coal combustion system can be categorized into two stages [11]. In the high-temperature combustion stage, Pb undergoes release from coal decomposition and oxidation, and retention in the solid phase facilitated by the mineral components in coal [12,13]. Subsequently, during the post-combustion stage, a portion of the released Pb is adsorbed or condensed onto fly ash during flue gas cooling, leading to its re-migration back to the solid phase [14]. It is crucial to probe the distinct transformation characteristics and key factors affecting Pb in each of these stages separately.

During the high-temperature combustion stage, coal exhibits substantial Pb release, with the release ratio varying considerably based on combustion conditions and the type of coal being burned [10,15–18]. Zhou et al. [15] found an increase in Pb release ratio from 14% to 28% as the combustion temperature rose in the range of 500–1000 °C. Xue et al. [16] conducted coal combustion experiments at 900–1300 °C and found that the release ratios of Pb in coal increased as the temperature increased. Similarly, Wang et al. [17] compared the Pb release ratios of four different coals when burned at 1150 °C, and found a range of 25–60% in Pb release ratios among them. These findings likewise indicate that there are differences in Pb release ratios for different coals, underscoring the complex of Pb transformation.

The variations observed in Pb transformation processes during high-temperature combustion are mainly influenced by the original forms of Pb and the mineral composition present in the coal. Pb in coal can be categorized as several forms according to its bonding with different minerals [13], namely carbonate- and oxide-bound, sulfide-bound, organic-bound, water-soluble and ion-exchangeable, and residual forms, with varying proportions among different coal types [13,19]. During combustion, the distribution of Pb within the solid phase undergoes changes. Ji et al. analyzed the solid combustion products of three types of coal at 900–1300 °C and found that the Pb remained in the solid phase basically existed in the residual form. Liu et al. [13] observed the release of Pb in different forms during the pyrolysis process at 300–1000 °C, different thermal stability of Pb with different forms. Moreover, Liu et al. [13] highlighted the generation of residual Pb in the pyrolysis products, indicating that in high-temperature combustion, Pb in each form not only undergoes release into the gas phase but also experiences mutual transformations. However, there are a limited number of reports addressing the transformation of Pb during biomass-coal blending combustion.

The release ratios of Pb vary among different coals, possibly due to the forms of Pb in the coal and the presence of inorganic components [20–30]. Minerals have demonstrated the ability to immobilize Pb

through external addition. SiO₂, Al₂O₃, bauxite, kaolin, acid clay and limestone can effectively adsorb PbO and PbCl₂ in the simulated flue gas, among which Kaolin has the strongest adsorption capacity [20–25]. Yao et al. [21] discovered that Si-Al-based minerals exhibit stronger adsorption capacity for PbCl₂ compared to Ca-based minerals at 800–1000 °C. Zhou et al. [15] observed SiO₂, Al₂O₃, Fe₂O₃, CaO, MgO, NaNO₃, and KNO₃ were capable of inhibiting Pb release at 500–1000 °C, particularly alkali metal compounds like KNO₃ and NaNO₃, which formed complexes with Pb to impede its release. However, Xu et al. [22] demonstrated that certain Na compounds (NaCl and Na₂CO₃) can promote As release by lowering the melting point of ash at 1000 °C. In straw, higher Si and Al contents also influenced the release of Pb at 700–1000 °C [24]. Apart from minerals, non-mineral components also influence the transformation of Pb [21,26–30]. Miller et al. [26] noted that HCl slightly promotes the release of Pb by generating a chloride compound (PbCl₂) with a lower melting and boiling point, while SO₂ promotes release of Pb by forming a sulfate compound (PbSO₄) with a higher melting and boiling point. Chemical equilibrium calculations conducted by Yao et al. [21] revealed that HCl reduces the dew point of Pb compounds, facilitating their release, while SO₂ increases the dew point of Pb compounds, inhibiting their release.

Biomass and coal differ in terms of their inorganic components. Specifically, biomass generally contains higher levels of K and Cl compared to coal [31–33]. These differing compositions may have an impact on the transformation of Pb. The reported effect of Cl is discussed in the above paragraph. K was also reported to affect Pb release during coal combustion. Zhou et al. [15] found that the addition of KNO₃ and NaNO₃ could inhibit the release of Pb by forming complexes with Pb at 500–1000 °C [15]. Xu et al. [22] showed that some Na compounds (NaCl, Na₂CO₃) could promote the release of As by lowering the ash melting point at 1000 °C. K compounds had also been proven to lower the melting point of coal ash [32,34]. Yao et al. [32] found that the addition of K₂CO₃ caused kyanite and mullite to react with potassium-containing minerals to form a low melting point eutectic. It was also found that KCl was able to react with CaSi₂ (melting point 1020 °C) to form low melting point SiO₂-Al₂O₃-K₂O eutectics (melting point 700–900 °C) [32]. Therefore, it is speculated that the high K content in biomass may also promote the release of Pb by lowering the ash melting point, which needs further exploration. Moreover, changes in K morphology during biomass combustion may also affect the role of K in Pb transformation. Xu et al. [22] discovered that Na can enhance the release of As from ash. Different forms of Na exhibit varying effects on As transformation, with Na₂CO₃ demonstrating a significantly stronger promotion effect compared to NaCl. However, the mechanisms through which different forms of K affect Pb transformation have yet to be reported in the literature.

The interaction of biomass and coal components during blending combustion might affect Pb emission. Therefore, the distribution characteristics and transformation pathways of Pb during biomass-coal blending combustion was studied in this research. Blending combustion experiments were carried out in a fixed-bed reactor at 1000, 1100, 1200 and 1300 °C, using coal and three different biomass samples (corn stalk, rice stalk, and bamboo flour). The release characteristics of Pb during blending combustion were obtained and the distribution of Pb forms was analyzed. To understand the influence of Cl and K components, HCl was introduced into the reactant gas, and the blending combustion experiments were conducted using fuels mixed with KCl or K₂CO₃. The analysis of microscopic morphology of solid combustion products, ash melting characteristics, and K retention were conducted to reveal the mechanisms underlying the impact of K components in biomass on Pb transformation. The results will support optimizing the combination of biomass and coal for blending combustion to control Pb emission.

2. Experimental

2.1. Sample

The selected biomasses consisted of herbaceous biomass (rice and corn stalks) and woody biomass (bamboo flour). The coal utilized originated from the Jingtai Power Plant, specifically power coal samples. Both the coal and biomass particles were sieved into 74–96 μm . Tables 1 and 2 present the results of the industrial and elemental analyses conducted on the coal and the three biomass types. Coal ash and biomass ash were respectively prepared according to GB/T212–2001 (Proximate analysis of coal) and GB/T28731–2012 (Proximate analysis of solid biofuels) of China [22]. The Cl contents in the raw coal and biomass were determined utilizing GB/T30729–2014 (Determination of chlorine in solid biofuels) and GB/T3558–2014 (Determination of chlorine in coal) of China. X-ray fluorescence spectroscopy (XRF) technique, specifically using the ARL PERFORM'X instrument from Thermo Fisher Scientific, USA, was employed to analyze the mineral components content in the ash. Formula (1) was used to calculate the concentration C_M (mg/g) of each mineral element in the raw coal and biomass, where M represents the mineral elements. The outcomes of these analyses are summarized in Table 3.

$$C_M = w_{MxOy} \times \frac{X \times MW_M}{MW_{MxOy}} \times A_{\text{ash}} \times 1000 \quad (1)$$

X and Y represent the number of M atom and O atom, respectively; w_{MxOy} represents the mass fraction (%) of the oxides of mineral M in ash; MW_M and MW_{MxOy} represent the relative atomic mass of mineral elements and the relative molecular mass of oxides, respectively; A_{ash} represents the fuel ash content (%).

Rice and corn stalks are typical examples of herbaceous biomasses, characterized by their elevated K and Cl contents. In contrast, woody biomass, specifically bamboo flour, exhibits relatively lower levels of K and Cl . The Pb content in the fuel was determined using an inductively coupled plasma optical emission spectrometer (ICP-OES; Leeman Labs Prodigy 7, USA). The results revealed a Pb content of 35.8 $\mu\text{g/g}$ in coal, 2.26 $\mu\text{g/g}$ in rice stalk, and levels below the detection limit in both corn stalk and bamboo flour.

For the experiments investigating the influence of K content and morphology on Pb transformation during combustion, high-purity K compounds, specifically KCl (CAS: 7447-40-7) and K_2CO_3 (CAS: 584-08-7), with a purity exceeding 99.8%, were procured from Sino-pharm Drugs. To simulate biomass-induced changes in sample layer thickness and promote dispersion of K compounds during combustion, cellulose (CAS:9004-34-6) from Aladdin was selected as the carrier for transporting the K compounds.

2.2. Experimental system

The biomass-coal blending combustion experiments were conducted using a fixed-bed reactor, as depicted in Fig. 1. The gas supply system on the left played a crucial role in delivering the required gases, namely N_2 , O_2 , and HCl , into the fixed-bed reactor. For the combustion experiments, a mixture of 79% N_2 and 21% O_2 was employed as the carrier gas. To investigate the influence of HCl on Pb release, N_2 was substituted with 500 ppm HCl gas, with N_2 serving as the equilibrium gas. The total gas flow rate was set at 500 mL/min and precisely regulated using a mass

Table 1
Proximate analysis of the coal and biomass samples (wt% ad).

sample	moisture	volatile	ash	fixed carbon
coal	3.1	28.1	19.5	49.3
rice stalk	3.6	64.0	15.8	16.6
corn stalk	4.8	69.8	7.3	18.1
bamboo flour	5.7	72.5	2.1	19.7

Table 2
Ultimate analysis of coal and biomass samples (wt% daf).

sample	C	H	O	N	S
coal	60.20	3.65	34.95	0.85	0.35
rice stalk	38.70	5.35	54.64	1.13	0.18
corn stalk	43.20	5.65	50.05	1.02	0.08
bamboo flour	47.00	5.99	46.64	0.36	0.01

Table 3
Contents of components in coal and biomass samples (mg/g ad).

sample	coal	rice stalk	corn stalk	bamboo flour
Si	20.67	34.27	7.77	2.57
Al	53.06	3.03	0.25	0.50
K	0.77	26.14	24.13	6.14
Ca	17.23	8.08	6.55	1.10
Fe	5.26	5.07	0.63	0.23
Mg	0.51	2.36	1.41	0.76
Na	0.13	1.74	0.04	0.18
Cl	0.14	9.90	6.42	1.33
$Pb(\times 10^{-3})$	35.80	2.26	0	0

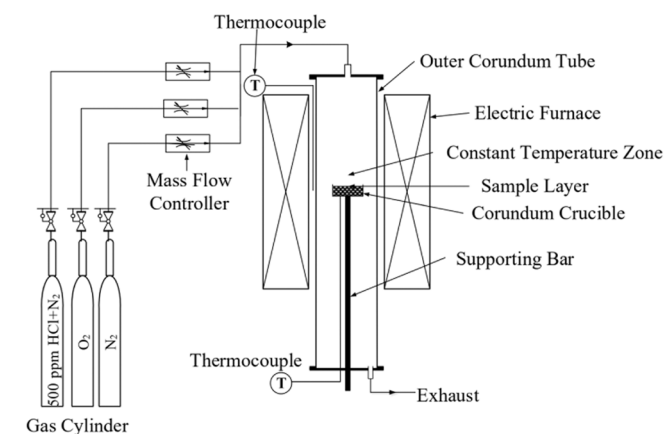


Fig. 1. Schematic of the fixed-bed reactor system.

flow controller (D08-1F, China). The fixed-bed reactor on the right side set up with a constant temperature zone. Once the atmosphere and temperature in the constant temperature zone reached the set point and stabilized, the crucible containing 0.8 g of the sample was placed in the constant temperature zone of the reactor using the supporting bar. After reaching the designated reaction time, the corundum crucible was carefully removed and allowed to cool before being collected for subsequent analysis.

2.3. Method

2.3.1. Combustion experiments

Fig. 2 showed the experimental flowchart of this study. The combustion experiments were carried out at temperatures of 1000, 1100, 1200 and 1300 $^{\circ}\text{C}$. In a preliminary experiment, the complete combustion time of each fuel was measured, and the concentrations of CO and CO_2 in the exhaust flue gas were determined using a Fourier transform infrared spectrometer (FTIR; Thermo Fisher Scientific Nicolet 6700, USA). The combustion process was considered complete when CO and CO_2 were not detected at the outlet. Based on this criterion, the fuels were burned for 55 min at 1000 $^{\circ}\text{C}$, resulting in a reduction of the CO and CO_2 concentrations to 0. Therefore, a reaction time of 55 min was selected for the experiments. The composition of the fuel samples under each operating condition is presented in Table 4. Since the biomass powder had a lower density compared to the coal

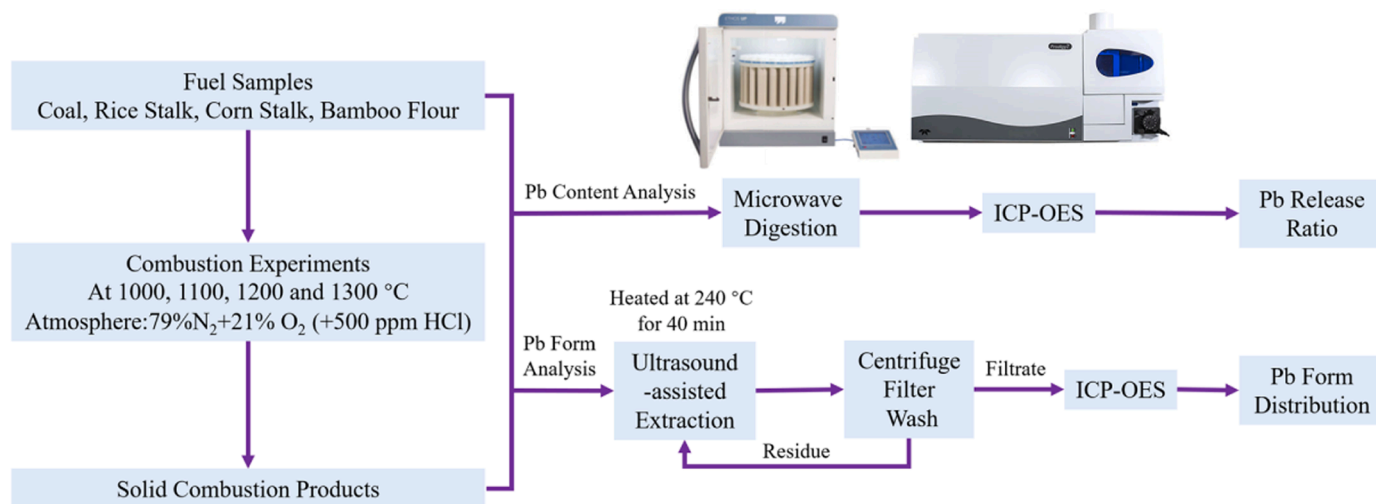


Fig. 2. Experimental flowchart.

Table 4

The compositions of fuel samples used in combustion experiments.

Sample	Proportion of raw materials
coal	100% coal
coa-cel	coal: cellulose = 1:1
coa-ric	coal: rice stalk = 1:1
coa-cor	coal: corn stalk = 1:1
coa-bam	coal: bamboo flour = 1:1
3coa-1cor	coal: corn stalk = 3:1
1coa-3cor	coal: corn stalk = 1:3
cc-HCl	coal: cellulose = 1:1 + 500 ppm HCl
cc-n%KCl (n = 1/3/5)	coal: cellulose = 1:1 + n wt% KCl (n wt% represents the mass fraction of element K)
cc-n%K ₂ CO ₃ (n = 1/3/5)	coal: cellulose = 1:1 + n wt% K ₂ CO ₃ (n wt% represents the mass fraction of element K)

powder, the sample layer of biomass-coal blending combustion experiment was thicker than coal combustion experiment without altering the total fuel mass. To ensure that variations in the sample layer thickness did not affect the experimental results, cellulose, which has a density similar to that of the biomass used in the experiments and contains only C, H, and O, was blended with coal. Each experimental case was repeated three times.

2.3.2. Distribution characteristics of Pb and K

To analyze the Pb content, the solid samples underwent microwave digestion using an ETHOS UP microwave digester (Milestone, Italy). The digestion procedure was as follows: approximately 50 mg of solid samples were weighed into the digestion tank, followed by the addition of 10 mL of HNO₃ (65.0–68.0%), 1 mL of H₂O₂ (30%), and 1 mL of HF (30%). The tank containing the samples was then placed into the microwave digester and heated to 240 °C for 40 min. After digestion, the concentration of Pb in the digestion solution was measured using ICP-OES. The Pb release ratio (R_f) during fuel combustion was calculated using Eq. (2).

$$R_f = \left(1 - \frac{c_{Pb,a}m_{a,f}}{c_{Pb,c}m_{c,f} + c_{Pb,b}m_{b,f}} \right) \times 100\% \quad (2)$$

$m_{c,f}$, $m_{b,f}$, and $m_{a,f}$ represent the mass of coal in the fuel sample, the mass of biomass in the fuel, and the mass of solid-phase combustion products, respectively, g. $c_{Pb,c}$, $c_{Pb,b}$, and $c_{Pb,a}$ represent the Pb content in coal, biomass, and solid-phase combustion products, respectively, $\mu\text{g/g}$.

To study the impact of K compounds on Pb transformation and analyze the relationship between Pb release and K retained in the solid combustion product, the retention of K (Re , mg) in the solid-phase combustion product of the K-containing cellulose-coal blending combustion was calculated. The K concentration in the digestion solution was measured using ICP-OES, and Re was determined by employing Eq. (3).

$$Re = c_{k,a}m_{a,f} \quad (3)$$

$m_{a,f}$ represents the mass of the solid-phase combustion product, and $c_{k,a}$ represents the K content of the solid-phase combustion product, mg/g.

A chemical extraction method [35] was utilized to analyze the forms of Pb. The classification of Pb forms and the corresponding extraction solutions used in each stage are provided in Table 5. The extraction procedure involved weighing 0.25 g of fuel or solid-phase combustion product in a centrifuge tube, followed by the addition of 15 mL of a 1 mol/L CH₃COONH₄ solution. Ultrasound was used to assist the extraction for a specific duration. After centrifugation, filtration, and washing, the filtrate was transferred to a new centrifuge tube for subsequent analysis. The Pb dissolved in the filtrate represented the water-soluble and ion-exchangeable Pb. The residue remaining after the first stage extraction was subjected to extraction with 15 mL of 3 mol/L HCl solution, 2 mol/L HNO₃ solution, and 2 mol/L HNO₃ + 30% H₂O₂ solution, in sequential order. The forms of Pb extracted at each stage are shown in Table 5. Any Pb remaining in the residue after these extractions was considered the residual Pb.

The Pb content in the filtrate was determined using ICP-OES, allowing for the calculation of the proportion of each form of Pb. To determine the proportion of each form of Pb in the coal, Eqs. (4) and (5) were utilized. The proportion of the residual form was obtained by subtraction.

Table 5

Extracts used for sequential chemical extraction.

Levels	Form of Pb	Extracts	Ultrasonic extraction temperature
1	Water-soluble and ion-exchangeable	1 mol/L CH ₃ COONH ₄	50 °C water bath heating
2	Carbonate- and oxide-bound	3 mol/L HCl	
3	Sulfide-bound	2 mol/L HNO ₃	
4	Organic-bound	2 mol/L HNO ₃ + 30% H ₂ O ₂	

$$PP_{c,i} = \left(\frac{M_{c,i}}{M_c} \right) \times 100\% \quad (4)$$

$$PP_{c,5} = 100\% - \sum_{i=1}^4 PP_{c,i} \quad (5)$$

$PP_{c,i}$ represents the proportion of Pb in level i form in coal (levels 1–4 are shown in Table 5, and level 5 represents the residual form, %). $M_{c,i}$ represents the mass of Pb in level i form in coal, μg . M_c represents the mass of Pb in coal, μg .

The proportion of each Pb form in the solid-phase combustion products was determined using Eqs. (6) and (7).

$$PP_{a,i} = \left(\frac{M_{a,i}}{M_{\text{raw}}} \right) \times 100\% \quad (6)$$

$$PP_{a,5} = 100\% - R - \sum_{i=1}^4 PP_{a,i} \quad (7)$$

$PP_{a,i}$ represents the proportion of Pb in level i form, %; $M_{a,i}$ represents the mass of Pb in level i form, μg ; M_{raw} represents the mass of Pb in the fuel, μg ; R represents the release ratio of Pb under the corresponding working conditions, %.

2.3.3. Ash melting characteristics

The ash melting point was determined using a microcomputer ash melting point tester (BYTHR-9 F, Boyuntian, China). The deformation temperature of ash was determined according to GB/T219–2008 (Determination of fusibility of coal ash) of China.

The surface morphology of the ash was characterized using scanning electron microscopy (SEM; Merlin, Zeiss, Germany).

3. Results and discussion

3.1. Distribution characteristics of Pb in fuels and solid combustion products

Combustion experiments were carried out at 1000–1300 °C to explore the effect of biomass-coal blending on Pb transformation by comparing the Pb release ratio and change in Pb form distribution with those of coal combustion. Fig. 3 illustrates the release ratios of Pb during coal combustion and blending combustion at temperatures ranging from 1000 °C to 1300 °C. The results demonstrate that with increasing combustion temperature, the release ratio of Pb in coal progressively rose. At 1000 °C, the release ratio was 64.2%, and reached 100% at 1300 °C. As the combustion temperature increased, the degree of ash melting increased. At 1300 °C, the degree of ash melting was high [22, 32], thus Pb was completely released into the gas phase. Cellulose exhibited a slight inhibitory effect on Pb release, with reductions of

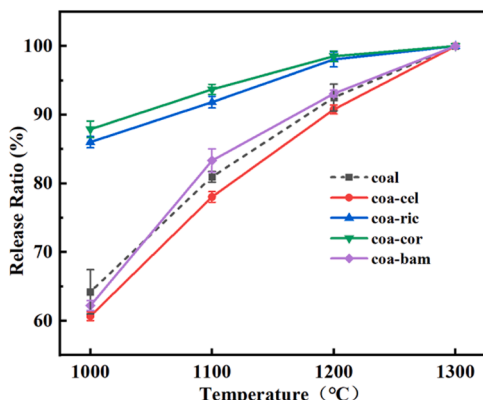


Fig. 3. Pb release ratios during coal combustion and blending combustion.

3.6%, 2.9%, and 1.7% at combustion temperatures of 1000, 1100, and 1200 °C, respectively. This was caused by a longer residence time of Pb in the cellulose-coal sample layer. Since the density of the cellulose was less than that of coal powder, the thickness of the sample layer increased when biomass and coal are blended at the same total mass. Hence the residence time of Pb in the sample layer was extended, and the contact with minerals was more complete, resulting in a decrease in the release ratio of Pb. In order to minimize the influence of sample layer thickness, the Pb release ratio during biomass-coal blending combustion should be compared with the Pb release ratio during coal-cellulose blending combustion, which have the similar sample layer thickness. In this comparison, all three types of biomass samples promoted Pb release. At 1000 °C, bamboo flour increased the release ratio from 60.7% to 62.2%. When the combustion temperature increased to 1100 °C and 1200 °C, the release ratios of Pb increased by 5.3% and 2.3%, respectively. Rice stalk led to significant increases in the release ratios of Pb, raising them from 60.7%, 78.0%, and 90.8% to 86.0%, 91.9%, and 98.1% at 1000, 1100, and 1200 °C, respectively. Similarly, corn stalk enhanced the release ratios of Pb to 87.9%, 93.7%, and 98.5%. The promoting effect can be understood by the change in the ash melting point [32]. At the same temperature, the solid product of biomass-coal blending combustion had a higher degree of melting, so the Pb release ratio was higher. It is evident that rice and corn stalks had comparable promotion effects on Pb release, while the promotion effect of the three biomasses followed the order: corn stalk \approx rice stalk > bamboo flour. The promoting effect decreased with the increasing combustion temperature. As the combustion temperature increased, on the one hand, the volatilization rate of K accelerated [36] and had less time to react with other minerals, thus the promotion effect of biomass weakened. On the other hand, as the temperature increased, the degree of ash melting increased, hence the Pb release ratios of all samples became closer and closer to 100%. By 1300 °C, the degree of ash melting was already very high, and the Pb in all samples was completely released into the gas phase.

Fig. 4 presents the release ratios of Pb during coal-corn stalk blending combustion at various blending ratios. It is observed that corn stalks exerted a significant influence on promoting the release of Pb from coal across all three blending ratios. Furthermore, the promotion effect on Pb release became more pronounced as the proportion of corn stalks in the fuel increased. At a combustion temperature of 1000 °C, when the mass fraction of corn stalk rose from 25% to 50% and 75%, the release ratio of Pb increased from 85.2% to 87.9% and 92.8%, respectively.

Table 6 illustrates the distribution of Pb forms in the fuel and its solid combustion products at temperatures ranging from 1000 °C to 1200 °C. The predominant forms of Pb were found to be carbonate- and oxide-bound (47.8% of total Pb), sulfide-bound (16.2% of total Pb), and residual forms (32.8% of total Pb). Upon combustion at 1000 °C, the sulfide-bound form nearly disappeared, and carbonate- and oxide-bound

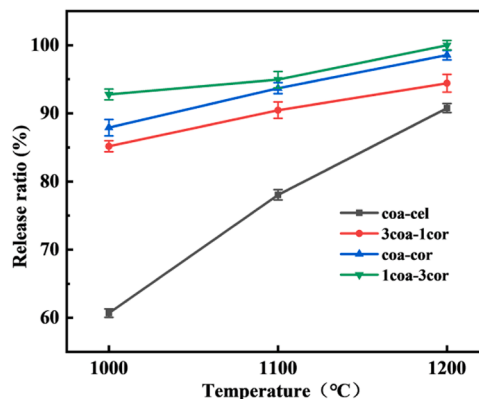


Fig. 4. Effects of coal-corn stalk blending ratio on Pb release during combustion.

Table 6
Distribution of Pb forms in the fuel and solid combustion products.

Sample	Water-soluble and ion-exchangeable bound	Carbonate- and oxide-bound	Sulfide-bound	Organic-bound	Residual
Fuel					
coal	1.48	47.79	16.16	1.79	32.78
Combustion Product at 1000 °C					
coal	0	1.18	0	0	34.59
coa-cel	0	1.35	0	0	37.97
coa-ric	0	2.63	0	0	11.34
coa-cor	0	0.64	0	0	11.46
coa-bam	0	0.75	0	0	37.01
cc-HCl	0	0.30	0	0	38.46
cc-3%KCl	0	0.74	0	0	4.56
cc-3%K ₂ CO ₃	0	1.52	0	0	0.32
at 1100 °C					
coal	0	1.07	0	0	17.99
coa-cel	0	0.64	0	0	21.31
coa-ric	0	0	0	0	8.15
coa-cor	0	0	0	0	6.31
coa-bam	0	0.51	0	0	16.05
cc-HCl	0	0	0	0	19.34
cc-3%KCl	0	0.84	0	0	5.91
cc-3%K ₂ CO ₃	0	0.81	0	0	0.07
at 1200 °C					
coal	0	0.71	0	0	6.77
coa-cel	0	0.41	0	0	8.82
coa-ric	0	0	0	0	1.93
coa-cor	0	0	0	0	1.47
coa-bam	0	0.02	0	0	6.91
cc-HCl	0	0	0	0	8.65
cc-3%KCl	0	0.69	0	0	7.93
cc-3%K ₂ CO ₃	0	1.48	0	0	0.10

Pb significantly decreased. Meanwhile, the proportion of residual Pb increased to 34.6%. As the combustion temperature increased to 1100 and 1200 °C, the proportions of carbonate- and oxide-bound Pb further decreased. Additionally, residual Pb decreased to 17.99% and 6.77%, respectively. Finally, at 1300 °C, all forms of Pb were completely released.

During coal-bamboo flour blending combustion, the proportions of residual Pb at 1000, 1100, and 1200 °C were 37.0%, 16.1%, and 6.91% of the total Pb in coal, respectively. During coal-rice stalk blending combustion, the residual Pb at 1000, 1100, and 1200 °C accounted for 11.3%, 8.15%, and 1.93% of the total Pb in coal, respectively. Moreover, a portion of Pb in the solid combustion products at 1000 °C was present in the form of carbonate- and oxide-bound, comprising 2.63%. For coal-corn stalk blending combustion, the residual Pb in the solid combustion products at 1000, 1100, and 1200 °C constituted 11.5%, 6.31%, and 1.47% of the total Pb in coal, respectively. Furthermore, a fraction of Pb at 1000 °C existed in the form of carbonate- and oxide-bound. Compared to the solid combustion products from coal alone, the blending solid combustion products exhibited a significant reduction in residual Pb. This indicates that biomass primarily enhanced the release ratio of Pb in coal by promoting the release of residual Pb.

During blending combustion, water-soluble and ion-exchangeable, sulfide-bound and organic-bound Pb in coal were thermally unstable and could be completely released at 1000 °C. Furthermore, carbonate-bound and oxide-bound Pb also experienced decomposition due to their thermal instability, resulting in a substantial decrease at 1000 °C and 1100 °C, and complete disappearance at 1200 °C. Interestingly, the proportion of residual Pb at 1000 °C was higher than that found in coal. This suggested a transformation of other forms of Pb into residual Pb during high-temperature combustion. This phenomenon occurred when Pb became incorporated into the aluminosilicate lattice or is enveloped by the aluminosilicate, thus remaining in a solid state as residue. Notably, when blending cellulose with coal during combustion, the proportions of residual Pb in the solid-phase combustion products were even higher. This can be attributed to the increased thickness of the material layer during cellulose-coal blending combustion, resulting in

an extended residence time for Pb and enhanced contact with silicon-aluminum minerals. As the temperature rose, the melting of silica-aluminate intensified, causing the decomposition and subsequent release of residual Pb [38]. Consequently, the proportion of residual Pb decreased and reached complete release at 1300 °C.

To summarize, when coal was blended with corn stalk, rice stalk, or bamboo flour, significant promotion of Pb release was observed. The promoting effect varied with biomass type. Increasing the proportion of biomass in the blending fuel enhanced Pb release. Biomass played a crucial role in promoting Pb release from coal, primarily by facilitating the release of residual Pb.

3.2. Effect of biomass components on Pb transformation during blending combustion

The promoting effect on Pb release varied with biomass samples. It was speculated that the difference in K and Cl contents in biomass affected the promotion. Comparing the inorganic components of the three biomasses used, the Cl contents of rice and corn stalks and bamboo flour were 0.990%, 0.642%, and 0.133%, respectively. Meanwhile, their K contents were 26.1 mg/g, 24.1 mg/g, and 6.14 mg/g, respectively. The ranking of the biomasses' promotion effect on Pb release, from strongest to weakest, was determined as corn stalk \approx rice stalk > bamboo flour. This variation in promotion effect was likely attributed to the K and Cl contents present in each biomass. To study the impact of K and Cl on Pb transformation, the combustion atmosphere was supplemented with HCl gas, or KCl and K₂CO₃ were added to the fuel.

In Fig. 5, the release ratio of Pb was depicted after introducing HCl gas into the combustion atmosphere during coal-cellulose blending combustion. The data reveals that at combustion temperatures of 1000, 1100, and 1200 °C, the increase in Pb release ratio were only 0.5%, 2.7%, and 0.6%, respectively. These findings indicate that the promotion effect of HCl on Pb release was not significant. Table 6 illustrates the distribution of Pb forms before and after the introduction of HCl gas into the combustion atmosphere. The results showed that HCl does not substantially alter the distribution of Pb forms.

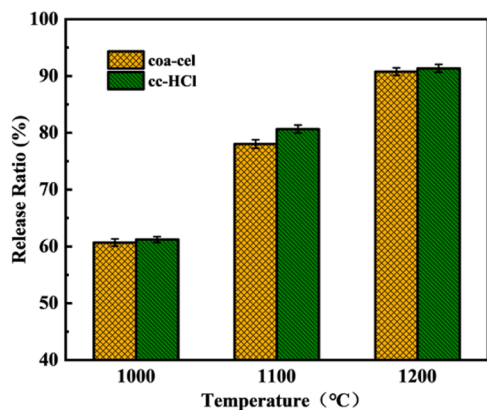


Fig. 5. Release ratio of Pb before/after introduction of HCl.

Fig. 6 displays the release ratio of Pb during K-containing cellulose-coal blending combustion. The addition of KCl and K_2CO_3 demonstrated a significant promotion effect on Pb release. The release ratio of Pb exhibited a positive correlation with the KCl content. For instance, at 1000 °C, as the mass fraction of K in the fuel increased from 0% to 1%, 3%, and 5%, the release ratios of Pb escalated from 60.7% to 86.9%, 94.7%, and 95.1%, respectively. Notably, fuels with different K contents exhibited varying degrees of temperature influence on the Pb release ratio. When the mass fractions of K were 1% and 5%, the release ratio of Pb notably increased as the combustion temperature rose from 1000 °C to 1100 °C. However, the increase in the release ratio of Pb became marginal when the combustion temperature further rose from 1100 °C to 1200 °C. Conversely, when the mass fraction of K in the fuel was 3%, the release ratio of Pb tended to decrease as the combustion temperature increased. This phenomenon can be attributed to the rapid volatilization of KCl in the fuel at higher temperatures, thereby weakening its role in promoting Pb release.

With an increasing addition ratio of K_2CO_3 , the release ratio of Pb gradually increased as well. When the addition ratio of K increased from 0% to 1%, the release ratio of Pb at 1000 °C, 1100 °C, and 1200 °C elevated from 60.7%, 78.0%, and 90.8% to 90.6%, 96.3%, and 98.7%, respectively. When the mass fractions of K in the fuel reached 3% and 5%, the release ratio of Pb exceeded 98% within the combustion temperature range of 1000–1200 °C. At this point, Pb was essentially completely released.

KCl and K_2CO_3 demonstrated distinct promotion effects on Pb release. When the mass fraction of K and combustion temperature remained constant, the promoting effect of K_2CO_3 on Pb release surpassed that of KCl. Previous studies have revealed that compared to NaCl, Na_2CO_3 exhibited more vigorous reactions with aluminosilicate

[22]. These reactions effectively reduced the ash melting point, thereby facilitating the release of Pb. K_2CO_3 was speculated to readily react with aluminosilicate, thereby promoting the release of Pb.

In Table 6, the alterations in the distribution of Pb forms in the solid combustion products are depicted before and after the addition of 3% K. The inclusion of KCl resulted in a reduction in the proportion of residual Pb from 38.0% and 21.3% to 4.56% and 5.91% at 1000 and 1100 °C, respectively. As the temperature reached 1200 °C, the proportion of residual Pb remained relatively unchanged before and after the addition of KCl. On the other hand, the addition of K_2CO_3 led to the near elimination of residual Pb within the temperature range of 1000–1200 °C. Less than 2% of Pb remained in the form of carbonate- and oxide-bound. These observations indicate that both KCl and K_2CO_3 promoted the release of residual Pb. Furthermore, the effect of K_2CO_3 exhibited greater strength compared to KCl.

To summarize, upon introducing HCl gas into the combustion atmosphere or incorporating KCl and K_2CO_3 into the fuels, the impact on the release of Pb was examined. The results indicate that HCl did not substantially influence the release of Pb. Conversely, both KCl and K_2CO_3 demonstrated a promotion effect on the release of residual Pb. Notably, the promoting effect of K_2CO_3 was found to be stronger than that of KCl.

3.3. Mechanism of Pb release promotion by K compounds

K compounds could promote the release of Pb in coal during biomass-coal blending combustion, and different K compounds have different effects. To further investigate the impact of K compounds on Pb transformation, an analysis of ash melting characteristics and K retention was conducted. Fig. 7 presents the surface morphology characterization results of the following: KCl-containing cellulose-coal blending combustion, K_2CO_3 -containing cellulose-coal blending combustion, and coal combustion products. Upon comparing (a), (b), and (c), notable distinctions could be observed. The surface of the coal combustion product appeared rough with numerous protrusions, and the particles exhibited irregular shapes. This indicates that when coal was combusted independently, the melting ratio of mineral components within the coal was low. However, with the addition of KCl and K_2CO_3 to the raw material, the shape of the solid-phase combustion product particles became more regular, and the surface became smoother. This observation suggests that melting occurred during blending combustion, causing fine particles to fuse together, forming larger particles. The presence of K compounds promoted particle melting during combustion and disrupted the stable aluminosilicate structure. Consequently, this promoted the release of residual Pb [37,38].

Fig. 8 displays the ash cone images obtained from the microcomputer ash melting point detector when different samples reached their respective softening temperatures. The results reveal that the

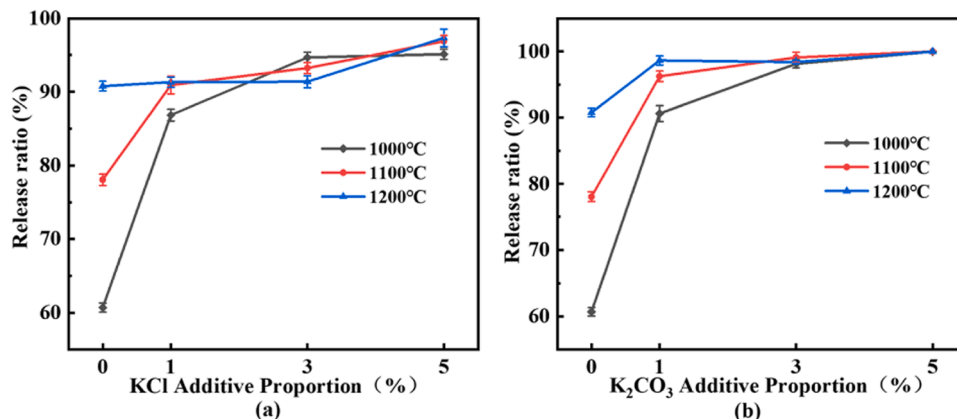


Fig. 6. Release ratios of Pb during blending combustion after addition of: (a) KCl (b) K_2CO_3 .

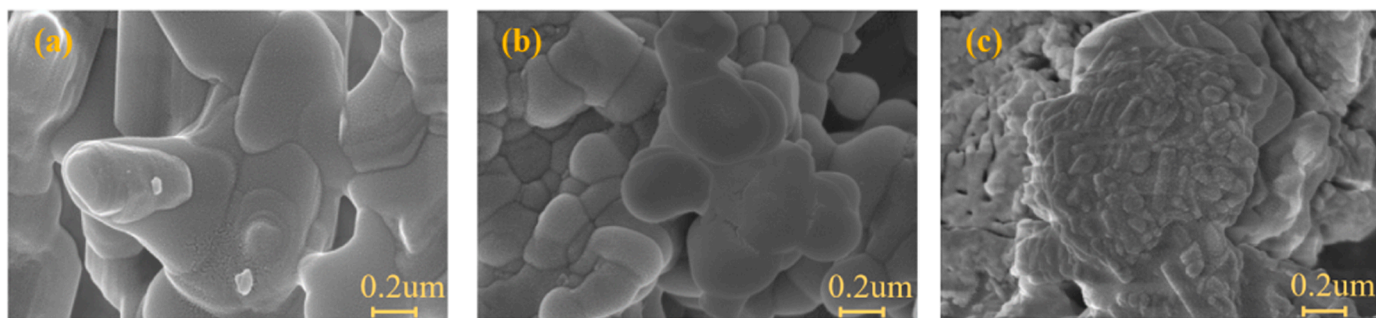


Fig. 7. Surface morphologies of different solid-phase combustion products: (a) coal+cellulose+KCl; (b) coal+cellulose+K₂CO₃; (c) coal+cellulose.

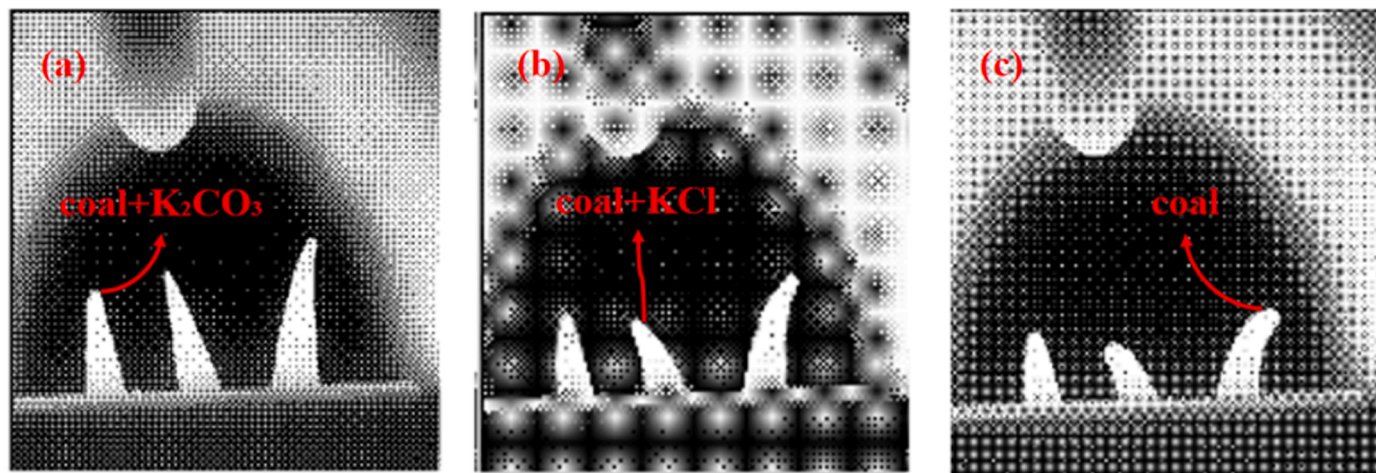


Fig. 8. Grey cone images of different fuels at 1398 °C, 1409 °C, 1417 °C.

deformation temperature of the K₂CO₃-containing cellulose-coal blending solid combustion product was 1398 °C, while that of the KCl-containing cellulose-coal blending combustion product was 1409 °C. In comparison, the coal combustion products exhibited a deformation temperature of 1417 °C. Using FactSage software, the liquid phase temperature T_L was calculated for various mass fractions of K₂O in the ash, namely 0.47% (coal ash), 1%, 3%, and 5%. Subsequently, the corresponding flow temperature FT was determined using the empirical formula $FT = -30 + 0.934 T_L$ [39]. The calculated results are presented in Table 7. It is evident that as the mass fraction of K₂O increased, the flow temperature gradually decreased. This indicates that the presence of K reduced the melting point of the ash, thereby promoting its melting. Furthermore, the softening temperature of the K₂CO₃-containing cellulose-coal blending combustion product was lower than that of the KCl-containing cellulose-coal blending combustion product. This suggests that the reaction between K₂CO₃ and aluminosilicate was more prone to occur. As a result, K₂CO₃ exhibited a stronger promoting effect compared to KCl.

In Section 3.2, it was observed that during KCl-containing cellulose-coal blending combustion, when the mass fraction of K in the fuel was 3%, the release ratio of Pb exhibited a decrease with an increase in combustion temperature. This phenomenon can be attributed to the accelerated volatilization rate of KCl as the temperature rose, resulting in reduced K retention in the solid phase. Consequently, the promotion

effect of K on the release of Pb became weaker. Although the increase in combustion temperature promoted the release of Pb, the accelerated volatilization of KCl weakened the promoting effect of K. In this case, the effect of K became greater than the effect of the temperature increase, leading to the above phenomenon. On the other hand, when the mass fraction of K was 1%, there was no significant change in the volatilization amount with temperature increase. For a mass fraction of K at 5%, the remaining KCl facilitated the almost complete release of Pb. In contrast to KCl, K₂CO₃ exhibited violent reactions with aluminosilicate. As a result, the accelerated volatilization rate caused by temperature increase had minimal impact on its promotion effect.

To validate this hypothesis, the retention of K in the solid combustion products was analyzed. Fig. 9 illustrates the variation in K retention in

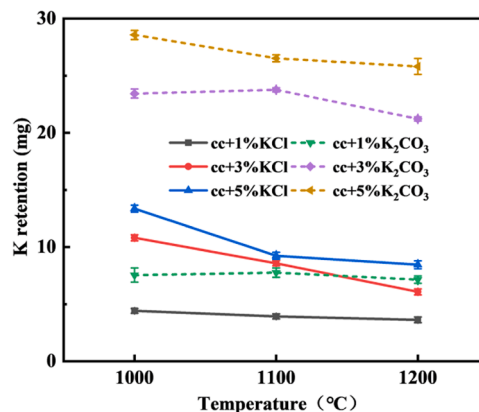


Fig. 9. K retention in blending combustion products.

Table 7
Liquid phase temperature and flow temperature at different K₂O mass ratio (°C).

K ₂ O ratio	0.47%	1%	3%	5%
T_L	1697.54	1694.69	1678.66	1654.34
FT	1555.50	1552.84	1537.86	1515.15

the solid-phase product during blending combustion. In KCl-containing cellulose-coal blending combustion, when the combustion temperature remained constant, the K retention in the solid combustion product exhibited a positive correlation with the K content in the raw material. Consequently, the release ratio of Pb increased with higher KCl content. When the KCl content in the raw material was consistent, the retention of K in the solid combustion products decreased as the combustion temperature increased. As a result, the promotion effect of K on the release of Pb from coal was weakened. During K_2CO_3 -containing cellulose-coal blending combustion, a positive correlation was observed between the K retention and the K content in the raw material. Similarly, when the K_2CO_3 content in the raw material remained constant, the K retention in the solid combustion product decreased with rising combustion temperature. Comparing the K retention between the blended KCl and K_2CO_3 combustion experiments, when other experimental conditions were the same, the K_2CO_3 -containing cellulose-coal blending combustion product exhibited significantly higher K retention compared to the KCl-containing cellulose-coal blending combustion product. This indicates that K_2CO_3 was more prone to react with aluminosilicates.

The mechanism of the influence of K compounds on Pb transformation was as follows. K compounds had the ability to react with aluminosilicates, disrupting their stable structure and reducing the ash melting point. This led to increased ash melting and facilitated the release of residual Pb, thus promoting the overall release of Pb from the coal. During biomass-coal blending combustion, the promotion effect was influenced by factors such as the K content in the biomass, the type of K compounds used, and the combustion temperature. When the temperature and type of K compounds were held constant, a higher K content in the biomass resulted in a stronger promotion effect. Similarly, when the content and type of K compounds were consistent, higher temperatures accelerate the volatilization rate of the K compound, thereby weakening its promotion effect. Lastly, when other experimental conditions were the same, the stronger promoting effect of K_2CO_3 compared to KCl could be attributed to its greater tendency to react with aluminosilicates.

In summary, biomass could promote the release of Pb in coal, and mainly promote the release of residual Pb. The promotion effect is related to the K and Cl content. HCl had almost no effect on Pb release, while K compounds could promote the release of Pb in the coal, and the promotion effect of K_2CO_3 was stronger than that of KCl. K compounds reduce the ash melting point mainly by reacting with aluminosilicates. This could destroy the stable aluminosilicate structure and release Pb that is encapsulated in the aluminosilicate or retained in the aluminosilicate lattice. Compared with KCl, K_2CO_3 was more likely to react with aluminosilicate and be retained. It had a stronger effect on promoting Pb release. These research results can help optimizing the selection of biomass and coal types for blending combustion. When the main forms of K in biomass are the same, choosing biomass with lower K content for blending combustion with coal can reduce the gas phase release of Pb. In addition, K compounds existed in different forms in biomass, and the proportions of each form in different biomass are different. Therefore, in order to reduce the gas phase release of Pb, when the K element content is close, biomass with KCl as the main form of K compound is more suitable for blending combustion with coal than biomass with K_2CO_3 as the main form of K compound. For coal with high Pb content, the proportion of biomass added should be reduced, or other mineral compounds which can capture Pb should be added into the blending combustion furnace to reduce Pb emission.

In addition to K_2CO_3 and KCl used in this study, K compounds also exist in other forms in biomass. Therefore, in future studies, the effects of other K compounds on Pb release can be further compared.

4. Conclusions

The transformation characteristics of Pb during biomass-coal blending combustion were obtained. When coal was blended with

corn stalk, rice stalk, or bamboo flour, significant promotion of Pb release was observed. At 1000, 1100, and 1200 °C, the Pb release ratio increased by 1.54–27.2%, 5.30–15.6% and 2.31–7.76%, respectively. Increasing the proportion of biomass in the fuel enhanced the promotion of Pb release.

Pb primarily existed in carbonate- and oxide-bound, sulfide-bound, and residual forms in coal. During combustion, these forms of Pb were thermally unstable and underwent form transformation or were released. The residual form was the dominant form of Pb in the solid combustion products. Biomass played a crucial role in promoting the release of Pb from coal, primarily by facilitating the release of residual Pb.

Different biomass had different promoting effects on Pb release, which is relevant to K and Cl contents in biomass. The influence of K and Cl components in biomass on Pb transformation was demonstrated. HCl was found to have minimal effect on the release or distribution of Pb in the product. On the other hand, both KCl and K_2CO_3 were observed to promote the release of Pb. K_2CO_3 exhibited a stronger promotion of Pb release compared to KCl. Both KCl and K_2CO_3 facilitated the release of residual Pb by reacting with aluminosilicates.

The mechanism through which K in biomass promoted the release of residual Pb was revealed. The addition of K compounds facilitated the melting of ash and destroyed the aluminosilicate structure, ultimately leading to the release of residual Pb. Notably, K_2CO_3 demonstrated a stronger ability to react with aluminosilicate and higher retention during blending combustion compared to KCl. Consequently, the promoting effect of K_2CO_3 on the release of Pb was more pronounced.

The findings of this study help understand the effect of biomass-coal blending combustion on Pb transformation and support optimizing the combination of biomass and coal for blending combustion to control Pb emission. In addition to K_2CO_3 and KCl studied in this study, K also exists in other compound forms in biomass, which needs further research to reveal their effect on Pb release.

Environmental implication

Utilizing biomass as fuel can reduce the emission of CO_2 , SO_2 , and NO_x . Biomass-coal blending combustion is an effective way to utilize biomass as fuel in large-scale. But heavy metal emission might be more severe in such a scenario. Pb is a typical harmful heavy metal in coal, whose emission causes serious environmental pollution. In this research, the promoting effect of K and Cl compounds in biomass on Pb release and the corresponding mechanism were revealed. The results are helpful for optimizing the selection of biomass and coal types to control Pb emission from the blending combustion source.

CRedit authorship contribution statement

Xing-yu Yang: Conceptualization, Methodology, Formal analysis, Investigation, Writing – original draft. **Guo-chang Song:** Methodology, Validation, Writing – review & editing, Resources, Visualization. **Zhong-wei Li:** Methodology, Validation, Writing – review & editing. **Qiang Song:** Writing – review & editing, Supervision, Project administration, Funding acquisition.

Declaration of Competing Interest

The authors declare that they have no known competing financial interests or personal relationships that could have appeared to influence the work reported in this paper.

Data availability

Data will be made available on request.

Acknowledgements

This work was financially supported by the China National Key Research and Development Program (2022YFC3701503) and the Fundamental Research Funds for the Central Universities of China (2022ZJFH04).

Appendix A. Supporting information

Supplementary data associated with this article can be found in the online version at [doi:10.1016/j.jhazmat.2023.132697](https://doi.org/10.1016/j.jhazmat.2023.132697).

References

- Zeng, T., Pollex, A., Weller, N., Lenz, V., Nelles, M., 2018. Blended biomass pellets as fuel for small scale combustion appliances: effect of blending on slag formation in the bottom ash and pre-evaluation options. *Fuel* 212, 108–116. <https://doi.org/10.1016/j.fuel.2017.10.036>.
- Niu, Y.Q., Tan, H.Z., Hui, S.E., 2016. Ash-related issues during biomass combustion: alkali-induced slagging, silicate melt-induced slagging (ash fusion), agglomeration, corrosion, ash utilization, and related countermeasures. *Prog Energy Combust* 52, 1–61. <https://doi.org/10.1016/j.pecs.2015.09.003>.
- Kim, J.H., Lee, Y.J., Yu, J.L., Jeon, C.H., 2019. Improvement in reactivity and pollutant emission by cofiring of coal and pretreated biomass. *Energy Fuel* 33 (5), 4331–4339. <https://doi.org/10.1021/acs.energyfuels.9b00396>.
- Sami, M., Annamalai, K., Wooldridge, M., 2001. Co-firing of coal and biomass fuel blends. *Prog Energy Combust* 27 (2), 171–214. [https://doi.org/10.1016/S0360-1285\(00\)00020-4](https://doi.org/10.1016/S0360-1285(00)00020-4).
- Krzyzanowski, M., 2008. WHO air quality guidelines for Europe. *J Toxicol Environ Health A* 71 (1–2), 47–50. <https://doi.org/10.1080/15287390701557834>.
- Zhao, Y.C., Yang, J.P., Ma, S.M., Zhang, S.B., Liu, H., Gong, B.G., et al., 2018. Emission controls of mercury and other trace elements during coal combustion in China: a review. *Int Geol Rev* 60 (5–6), 638–670. <https://doi.org/10.1080/00206814.2017.1362671>.
- Song, G.C., Xu, W.T., Yang, X.Y., Song, Q., 2023. Process analysis of Pb transformation in the coal devolatilization stage. *Fuel* 340, 127549. <https://doi.org/10.1016/j.fuel.2023.127549>.
- Ito, S., Yokoyama, T., Asakura, K., 2006. Emissions of mercury and other trace elements from coal-fired power plants in Japan. *Sci Total Environ* 368 (1), 397–402. <https://doi.org/10.1016/j.scitotenv.2005.09.044>.
- Wang, J.W., Zhang, Y.S., Liu, Z., Gu, Y.Z., Norris, P., Xu, H., et al., 2019. Coefficient of air pollution control devices on trace element emissions in an ultralow emission coal-fired power plant. *Energy Fuel* 33 (1), 248–256. <https://doi.org/10.1021/acs.energyfuels.8b03549>.
- Zajac, G., Szyszlak-Barglowicz, J., Szczepanik, M., 2019. Influence of biomass incineration temperature on the content of selected heavy metals in the ash used for fertilizing purposes. *Appl Sci-Basel* 9 (9), 1790. <https://doi.org/10.3390/app9091790>.
- Seames, W.S., Wendt, J.O.L., 2000. Partitioning of arsenic, selenium, and cadmium during the combustion of Pittsburgh and Illinois #6 coals in a self-sustained combustor. *Fuel Process Technol* 63 (2–3), 179–196. [https://doi.org/10.1016/S0378-3820\(99\)00096-X](https://doi.org/10.1016/S0378-3820(99)00096-X).
- Zhang, J., Han, C.L., Xu, Y.Q., 2003. The release of the hazardous elements from coal in the initial stage of combustion process. *Fuel Process Technol* 84 (1–3), 121–133. [https://doi.org/10.1016/S0378-3820\(03\)00049-3](https://doi.org/10.1016/S0378-3820(03)00049-3).
- Liu, R.Q., Zhang, X.L., Wang, J.W., Wang, T.J., Xie, J.F., 2014. Transformation behaviors of lead during thermal treatment of Heidaigou coal. *Energy Source Part A* 36 (12), 1366–1371. <https://doi.org/10.1080/15567036.2011.553660>.
- Seames, W.S., 2003. An initial study of the fine fragmentation fly ash particle mode generated during pulverized coal combustion. *Fuel Process Technol* 81 (2), 109–125. [https://doi.org/10.1016/S0378-3820\(03\)00006-7](https://doi.org/10.1016/S0378-3820(03)00006-7).
- Zhou, C.C., Liu, G.J., Xu, Z.Y., Sun, H., Lam, P.K.S., 2018. Retention mechanisms of ash compositions on toxic elements (Sb, Se and Pb) during fluidized bed combustion. *Fuel* 213, 98–105. <https://doi.org/10.1016/j.fuel.2017.10.111>.
- Xue, Z.Y., Dong, L., Zhong, Z.P., Lai, X.D., Huang, Y.J., 2021. Capture effect of Pb, Zn, Cd and Cr by intercalation-exfoliation modified montmorillonite during coal combustion. *Fuel* 290, 119980. <https://doi.org/10.1016/j.fuel.2020.119980>.
- Wang, J., Tomita, A., 2003. A chemistry on the volatility of some trace elements during coal combustion and pyrolysis. *Energy Fuel* 17 (4), 954–960. <https://doi.org/10.1021/ef020251o>.
- Song, G.C., Xu, W.T., Ji, P., Song, Q., 2019. Study on the transformation of arsenic and lead in Pyrite during thermal conversion. *Energy Fuel* 33 (9), 8463–8470. <https://doi.org/10.1021/acs.energyfuels.9b02028>.
- Ji, P., Song, G.C., Xu, W.T., Song, Q., 2019. Transformation characteristics of arsenic and lead during coal combustion. *Energy Fuel* 33 (9), 9280–9288. <https://doi.org/10.1021/acs.energyfuels.9b02189>.
- Wang, X.Y., Huang, Y.J., Pan, Z.G., Wang, Y.X., Liu, C.Q., 2015. Theoretical investigation of lead vapor adsorption on kaolinite surfaces with DFT calculations. *J Hazard Mater* 295, 43–54. <https://doi.org/10.1016/j.jhazmat.2015.03.020>.
- Yao, H., Naruse, I., 2009. Using sorbents to control heavy metals and particulate matter emission during solid fuel combustion. *Particology* 7 (6), 477–482. <https://doi.org/10.1016/j.partic.2009.06.004>.
- Xu, W.T., Song, G.C., Hu, K.X., Song, Q., Yao, Q., 2021. The redistribution of arsenic during the interaction between high-temperature flue gas and ash. *Fuel Process Technol* 212, 106641. <https://doi.org/10.1016/j.fuproc.2020.106641>.
- Yu, S.H., Zhang, C., Ma, L., Fang, Q.Y., Chen, G., 2021. Experimental and DFT studies on the characteristics of PbO/PbCl₂ adsorption by Si/Al-based sorbents in the simulated flue gas. *J Hazard Mater* 407, 124742. <https://doi.org/10.1016/j.jhazmat.2020.124742>.
- Sommersacher, P., Kienzl, N., Brunner, T., Obernberger, I., 2016. Simultaneous online determination of S, Cl, K, Na, Zn, and Pb release from a single particle during biomass combustion. part 2: Results from test runs with spruce and straw pellets. *Energy Fuel* 30 (4), 3428–3440. <https://doi.org/10.1021/acs.energyfuels.5b02766>.
- Zhang, A.J., Liu, J., Zhang, Z., Yang, Y.J., Yu, Y.N., Zhao, Y.C., 2021. Insights into the mechanism of lead species adsorption over Al₂O₃ sorbent. *J Hazard Mater* 413, 125371. <https://doi.org/10.1016/j.jhazmat.2021.125371>.
- Miller, B., Dugwell, D.R., Kandiyoti, R., 2003. The influence of injected HCl and SO₂ on the behavior of trace elements during wood-bark combustion. *Energy Fuel* 17 (5), 1382–1391. <https://doi.org/10.1021/ef030020x>.
- Li, R.D., Zhao, W.W., Li, Y.L., Wang, W.Y., Zhu, X., 2015. Heavy metal removal and speciation transformation through the calcination treatment of phosphorus-enriched sewage sludge ash. *J Hazard Mater* 283, 423–431. <https://doi.org/10.1016/j.jhazmat.2014.09.052>.
- Jiao, F., Cheng, Y., Zhang, L.A., Yamada, N., Sato, A., Ninomiya, Y., 2011. Effects of HCl, SO₂ and H₂O in flue gas on the condensation behavior of Pb and Cd vapors in the cooling section of municipal solid waste incineration. *P Combust Inst* 33, 2787–2793. <https://doi.org/10.1016/j.proci.2010.07.062>.
- Zhong, Z.P., Li, J.F., Ma, Y.Y., Yang, Y.X., 2021. The adsorption mechanism of heavy metals from coal combustion by modified kaolin: experimental and theoretical studies. *J Hazard Mater* 418, 126256. <https://doi.org/10.1016/j.jhazmat.2021.126256>.
- Zhao, S.L., Duan, Y.F., Li, Y.N., Liu, M., Lu, J.H., Ding, Y.J., et al., 2018. Emission characteristic and transformation mechanism of hazardous trace elements in a coal-fired power plant. *Fuel* 214, 597–606. <https://doi.org/10.1016/j.fuel.2017.09.093>.
- Chen, C., Luo, Z.Y., Yu, C.J., 2019. Release and transformation mechanisms of trace elements during biomass combustion. *J Hazard Mater* 380, 120857. <https://doi.org/10.1016/j.jhazmat.2019.120857>.
- Yao, X.W., Zhou, H.D., Xu, K.L., Xu, Q.W., Li, L., 2019. Evaluation of the fusion and agglomeration properties of ashes from combustion of biomass coal and their mixtures and the effects of K₂CO₃ additives. *Fuel* 255, 115829. <https://doi.org/10.1016/j.fuel.2019.115829>.
- Vassilev, S.V., Vassileva, C.G., Song, Y.C., Li, W.Y., Feng, J., 2017. Ash contents and ash-forming elements of biomass and their significance for solid biofuel combustion. *Fuel* 208, 377–409. <https://doi.org/10.1016/j.fuel.2017.07.036>.
- Yao, X.W., Zheng, Y., Zhou, H.D., Xu, K.L., Xu, Q.W., Li, L., 2020. Effects of biomass blending, ashing temperature and potassium addition on ash sintering behaviour during co-firing of pine sawdust with a Chinese anthracite. *Renew Energy* 147, 2309–2320. <https://doi.org/10.1016/j.renene.2019.10.047>.
- Finkelman, R.B., Palmer, C.A., Wang, P.P., 2018. Quantification of the modes of occurrence of 42 elements in coal. *Int J Coal Geol* 185, 138–160. <https://doi.org/10.1016/j.coal.2017.09.005>.
- Xue, Z.Y., Zhong, Z.P., Zhang, B., Zhang, J., Xie, X.W., 2017. Potassium transfer characteristics during co-combustion of rice straw and coal. *Appl Therm Eng* 124, 1418–1424. <https://doi.org/10.1016/j.applthermaleng.2017.06.116>.
- Zhao, H.B., Xu, W.T., Song, Q., Zhuo, J.K., Yao, B., 2018. Effect of steam and SiO₂ on the release and transformation of K₂CO₃ and KCl during biomass thermal conversion. *Energy Fuel* 32 (9), 9633–9639. <https://doi.org/10.1021/acs.energyfuels.8b02269>.
- Xu, W.T., Song, G.C., Song, Q., Yao, Q., 2022. Study on the mechanism of lead release from ash under the action of high-temperature flue gas. *Fuel Process Technol* 227, 107089. <https://doi.org/10.1016/j.fuproc.2021.107089>.
- Jak, E., 2002. Prediction of coal ash fusion temperatures with the F^{*}A^{*}C^{*}T thermodynamic computer package. *Fuel* 81 (13), 1655–1668. [https://doi.org/10.1016/S0016-2361\(02\)00091-1](https://doi.org/10.1016/S0016-2361(02)00091-1).